[4] M. Sadakane, M. H. Dickman, M. T. Pope, *Angew. Chem.* **2000**, *112*, 3036; *Angew. Chem. Int. Ed.* **2000**, *39*, 2914.
[5] Y3, Y4, and W13 of **R** belong to three different edge-shared $Y(3,4)W_2O_{12}$ and $W(13)W_2O_{13}$ groups and are linked to the others through corner-shared oxygen atoms to give an A-type positional isomer. The fourth edge-shared W_3O_{13} group is not rotated with respect to the parent α-Keggin part (see Supporting Information); this defines the second type of isomerism as α.
[6] A detailed description of the bonding in **L** and **R** (Figure 2) follows: Y1 (7-coordinate) and Y2 (8-coordinate) are both bound to oxygen atoms of **L**. Y1 is also bound to one oxygen atom in each of the symmetry-equivalent **L** (μ_2-O (2.264(17) Å) to W10A) and **R** (μ_2-O (2.275(19) Å) to W13A) and μ_2-O (2.301(17) Å) to W12. The other four coordination sites of the eight-coordinate Y2, which connect **L** to **R**, are occupied by μ_3-O (2.483(17) Å) to Y3 and Y4, μ_2-O to W12 (2.310 Å), μ_2-O to W11 (2.39 Å) and a terminal O atom (2.44 Å). Similarly, Y3 and Y4 are bound to O atoms of **R**. Y3 is connected to **L** by μ_3-O (2.442(17) Å) to W4 and W5, μ_3-O (2.556(18) Å) to W5 and W10, μ_3-O (2.464 (18) Å) to W4 and Y2, and the fourth remaining site to μ_3-O (2.337(17) Å) to Y2 and Y4. The three remaining coordination sites on Y4, connecting Y4 to **L**, are occupied by μ_2-O (2.341(18) Å) to W12, μ_2-O (2.368(19) Å) to W11, and μ_3-O (2.335(17) Å) to W12 and Y2.
[7] A. Müller, F. Peters, M. T. Pope, D. Gatteschi, *Chem. Rev.* **1998**, *98*, 239, and references therein; W. H. Knoth, P. J. Domaille, R. L. Harlow, *Inorg. Chem.* **1986**, 1577.
[8] For example, reaction of uranyl ion with $Na_7[NaAs_4W_{40}O_{140}]\cdot 60H_2O$, a source of $AsW_9O_{33}^{9-}$, resulted in rearrangement to form species that contain 3 or 2 $AsW_{10}O_{36}^{9-}$ units, depending on pH. The uranyl ion has specific stereochemical requirements that result in interlinking of $AsW_9O_{33}^{9-}$ and $AsW_{10}O_{36}^{9-}$ units. K.-C. Kim, M. T. Pope, *J. Chem. Soc. Dalton Trans.* **2001**, 986. Counterions also were found to play an important structural role in the reaction of uranyl ion with $PW_9O_{34}^{9-}$: K.-C. Kim, M. T. Pope, *J. Am. Chem. Soc.* **1999**, *121*, 8512.
[9] S. M. Gorun, G. C. Papaefthymiou, R. B. Frankel, S. J. Lippard, *J. Am. Chem. Soc.* **1987**, *109*, 3337. For Y^{III}: O26, Y3, W5, W10: 325.65; O46, Y2, Y3, Y4: 341.0; O25, Y2, Y3, W4: 345.38. For Eu^{III}: O46, Eu2, W11, W17: 329.18; O33, Eu1, Eu2, Eu4: 338.30; O45, Eu2, Eu4, W16: 341.92.
[10] Y^{III}–μ_3-O, Y^{III}–μ_2-O, Y^{III}–O, Y^{III}–OH_2 bonds: a) E. H. Barash, P. S. Coan, E. B. Lobkovsky, W. E. Streib, K. G. Caulton, *Inorg. Chem.* **1993**, *32*, 497; b) B. M. Chamberlain, Y. Sun, J. R. Hagadorn, E. W. Hemmesch, V. G. Young, Jr., M. Pink, M. A. Hillmyer, W. B. Tolman, *Macromolecules*, **1999**, *32*, 2400; c) F. A. Cotton, P. Legzdins, *Inorg. Chem.* **1968**, *7*, 1777. Gd^{III}/Tb^{III} bonds to μ_3-O, μ_2O, O, OH_2: d) X.-M. Chen, Y.-L. Wu, Y.-X. Tong, Z. Sun, D. N. Hendrickson, *Polyhedron* **1997**, *16*, 4265; e) J. C. Plakatouras, I. Baxter, M. Hursthouse, K. M. A. Malik, J. McAleese, S. R. Drake, *J. Chem. Soc. Chem. Commun.* **1994**, 2455; f) O. Poncelet, L. G. Hubert-Pfalzgraf, *Polyhedron* **1989**, *8*, 2183; g) R. Wang, M. D. Carducci, Z. Zheng, *Inorg. Chem.* **2000**, *39*, 1836; h) J. Liu, E. A. Meyers, S. G. Shore, *Inorg. Chem.* **1998**, *37*, 5410.
[11] M. S. Weeks, C. L. Hill, R. F. Schinazi *J. Med. Chem.* **1992**, *35*, 1216.
[12] W. DeW. Horrocks, Jr., D. R. Sudnick, *J. Am. Chem. Soc.* **1979**, *101*, 334.
[13] W. G. Klemperer, *Inorg. Synth.* **1992**, *27*, 71.
[14] G. M. Sheldrick, SHELXTL, An integrated system for solving, refining and displaying crystal structures from diffraction data, University of Göttingen, Germany, **1981**.

"Nanoobjects" by Self-Assembly Concomitant with Modifications under Alterable Boundary Conditions: Incorporation of Paramagnetic Metal Centers (Cu^{2+}) in Ring-Shaped Molybdenum-Oxide Based Clusters**

Achim Müller,* Erich Krickemeyer, Hartmut Bögge, Marc Schmidtmann, Paul Kögerler, Christina Rosu, and Eike Beckmann

Dedicated to Professor Dr. Hansgeorg Schnöckel on the occasion of his 60th birthday

Until now it has been a tremendous and ongoing challenge to initiate a variety of chemical reactions at *well-defined* positions even of the same and structurally *well-defined* nanoobject, especially if significant property changes or novel functionalities are intended.[1] This aim has now been achieved for giant ring-shaped molybdenum oxide based clusters of the type $\{Mo_{154}\}$ and $\{Mo_{176}\}$ which can be obtained in related crystalline salts in a facile high-yield synthesis and exhibit nanosized cavities, a variety of sites with different well-defined functional groups, and overall are comparable to a nanostructured landscape.[2, 3] Here we report the incorporation of paramagnetic metal centers, that is, Cu^{2+} ions, in cavities of these rings—which are spanned by four O atoms and have the corresponding appropriate size—according to a basic type of self-assembly process leading to nanoobjects all of which have the ring topology. Important in this context is that this allows a variety of deliberate concomitant modifications under alterable boundary conditions—such as the pH, temperature, and/or presence of different substrates—corresponding to the different sites.[4] The procedure opens perspectives not only for a new type of nanochemistry but also for an understanding of a basic reaction type of material organization (see below).

The reduction of an acidified aqueous polymolybdate solution with copper powder leads to the crystalline black compound **1**, which was characterized by elemental analyses

$$(NH_4)_{26}[(H_4Cu^{II}_5)Mo^{V}_{28}Mo^{VI}_{114}O_{432}(H_2O)_{58}]\cdot\approx 300\,H_2O \qquad \mathbf{1}$$

(including cerimetric titration to determine the formal number of Mo^V centers), thermogravimetry (to determine the amount of crystal water), spectroscopy (UV/Vis/NIR, infrared (IR), resonance-Raman, ESR), single-crystal X-ray structure analysis,[5] and bond valence sum (BVS)[6] calculations (to determine the positions of the H_2O molecules and to

[*] Prof. Dr. A. Müller, E. Krickemeyer, Dr. H. Bögge, M. Schmidtmann, Dr. P. Kögerler, Dr. C. Rosu, Dipl.-Chem. E. Beckmann
Lehrstuhl für Anorganische Chemie I
Fakultät für Chemie der Universität
Postfach 100131, 33501 Bielefeld (Germany)
Fax: (+49) 521-106-6003
E-mail: a.mueller@uni-bielefeld.de

[**] The authors thank Prof. D. Gatteschi, University of Florence (Italy), for helping with the interpretation of the ESR spectrum, and Dipl.-Chem. A. Berkle and Dr. J. Hockemeyer, University of Bielefeld (Germany), for their collaboration. C. R. thanks the Alexander von Humboldt Foundation for her fellowship. Financial support by the Deutsche Forschungsgemeinschaft and the Fonds der Chemischen Industrie is gratefully acknowledged.

  0044-8249/01/11321-4158 $ 17.50+.50/0

distinguish between the Mo^{VI} and Mo^{V} centers) as well as magnetic susceptibility measurements.

The crystal structure shows the abundance of the cluster anions $[\{Mo_8^{V/VI}O_{26}(\mu_3O)_2X_i(H_2O)_3Mo^{V/VI}\}_{14}\{Mo_2^{VI}O_5(H_2O)_2\}_8]^{26-}$ ($\Sigma X_i = 4H + 5Cu$) (**1a**) which are derivatives of the aforementioned prototypal tetradecameric $\{Mo_{154}\} \equiv \{Mo_8\}_{14}\ \{Mo_1\}_{14}\ \{Mo_2\}_{14}$ **2a** type species.[2, 3] In comparison to the $\{Mo_{154}\}$ anion, **1a** lacks six $\{Mo_2\}$-type building blocks and shows fascinating novel features: In the tetrahedral cavities spanned by four oxygen atoms (two μ_3 and two terminal, abundant and within the $\{Mo_8\}$ building blocks)—that is, at well-defined sites underneath the cluster surface—five Cu^{2+} centers are incorporated, but interestingly are not uniformly distributed in the cavities, the largest occupation number being 0.73. These replace some of the 14 H atoms of the parent cluster **2a** which are bonded to one of the two above-mentioned μ_3-O atoms that form the cavities (Figure 1). Whereas with high H^+ ion concentrations the maximum 14-fold protonation of the tetradecameric cluster is obtained,[3] an increased pH value—here because of buffering with $HCOONH_4$—leads to lower degrees of protonation and to Cu^{2+} coordination to the basic μ_3-O atoms.

Whereas the resonance-Raman ($\lambda_e = 1064$ nm excitation line) and IR spectra are nearly identical with that of the parent cluster **2a**, the electronic spectrum of solid **1** shows, as a result of the abundance of Cu^{2+} centers, an additional band at ≈ 520 nm and a blue shift of the higher energy intervalence charge transfer (IVCT) transition, localized in the $Mo_5^{V/VI}O_6$-type compartments (see ref. [3]), each of which contains two delocalized Mo (4d) electrons. The change of the charge transfer is caused by the fact that the encapsulated Cu^{2+} ions are coordinated to the μ_3-O atoms which belong to the Mo_5O_6 compartments and therefore influence the electronic structure/distribution. Furthermore, the room-temperature ESR powder spectrum (Figure 2)—which is similar to that of tetrahedral complexes containing CuX_4 and in particular CuO_4 groups[7, 8]—shows nicely the abundance of the $Cu^{2+}(d^9)$

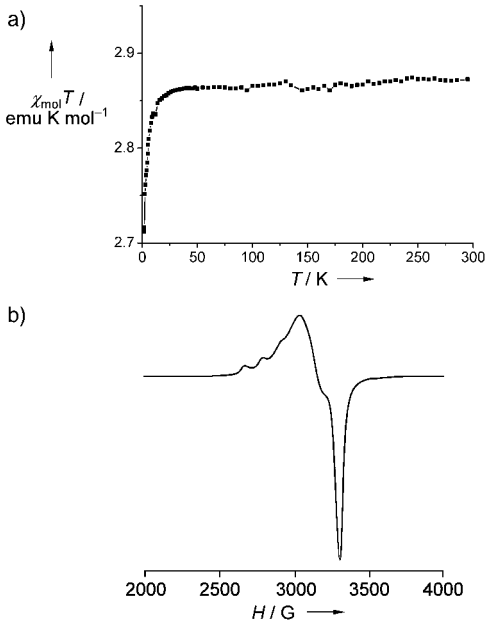

Figure 2. Magnetic susceptibility as function of temperature (a) and ESR spectrum, X-band, room temperature (b) of solid **1**.

centers with the characteristic $g_x = 2.07$, $g_y = 2.15$, and $g_z = 2.37$, and a hyperfine splitting constant $A_z = 125$ G (because of the nuclear spin of $^{63/65}Cu$ with $I = 3/2$), thus showing that the $Cu^{2+}\cdots Cu^{2+}$ magnetic interactions ($Cu\cdots Cu \approx 6.2$ Å) are practically negligible (see also ref. [7]). This observation is also supported by the measured susceptibility data (Figure 2). Upon correction of the diamagnetic and temperature independent paramagnetism (TIP) contributions (that sum up to -2.5×10^{-4} emu mol^{-1}), $\chi_{mol}T$ at high temperatures displays a constant value of approximately 2.86 emu K mol^{-1} at a plateau which corresponds to around 6 Cu^{2+} centers per formula unit for $g = 2.2$ (compare with ESR results). Accordingly there is a small error limit of ± 1 in the number of Cu atoms while one more Cu^{2+} ion can directly replace 2 NH_4^+ ions in the lattice or can be localized in the cluster anion. (The number of Cu atoms in the formula corresponds to the sum of their occupation factors.) The observed antiferromagnetic cou-

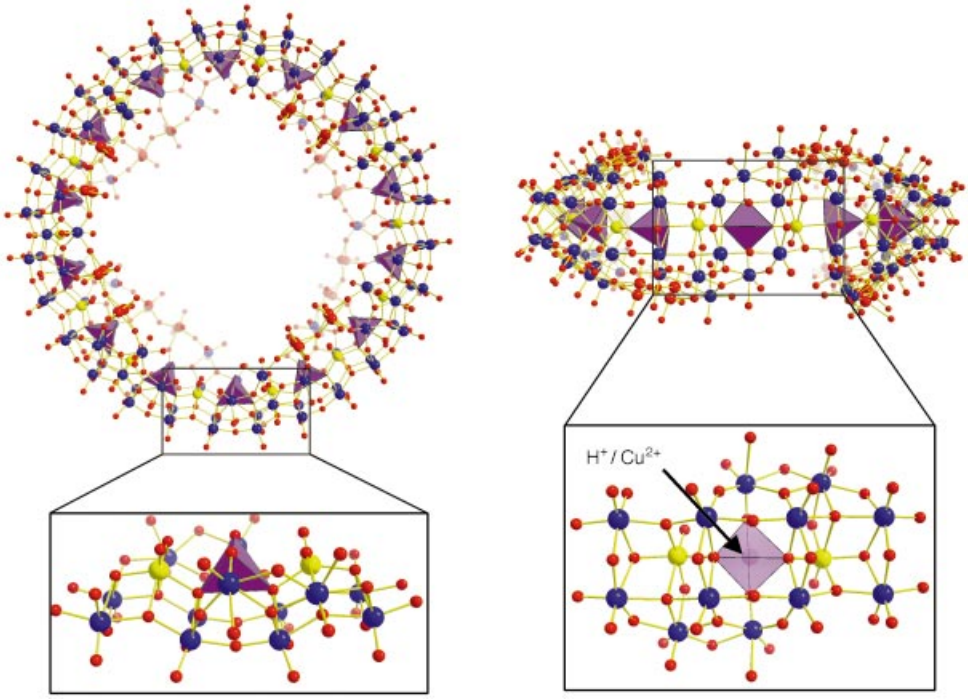

Figure 1. Molecular structure of the cluster anion **1a** (top and side view) in crystals of **1** in ball and stick representation while the O_4 (Cu) tetrahedra (violet) are given in polyhedral representation; additionally, one relevant segment is highlighted separately.

  0044-8249/01/11321-4159 $ 17.50+.50/0

pling interactions—of inter- and intramolecular nature—are very weak and the susceptibility can be modeled using a Curie–Weiss term with a very low Weiss temperature of $\theta \approx -0.5$ K. Consequently, $\chi_{mol}T$ decreases only below about 20 K.

Interestingly, the thermogravimetric analysis shows that it is possible to remove most of the crystal water by heating **1** to around 300 °C (weight loss approximately 20 %), and thus in principle(!) to generate a mesoporous magnetic material. This is new for this type of wheel-shaped clusters since to date we have never succeeded in isolating pure salts with NH_4^+ ions which may be easily decomposed on heating; important in this context: crystal water molecules in the channels are fixed by the cations.[8] (According to the IR spectrum the compound heated to 300 °C does not contain NH_4^+ ions.)

The remarkable integration of the paramagnetic Cu^{2+} ions into the cluster cavities under certain self-assembly conditions leading to the giant wheel-type parent species is possible because the dimensions of the aforementioned O_4-type cavities in **2a** provide the exact characteristic Cu–O distances (2.0 ± 0.1 Å). The assembly route leads in principle from the simple mononuclear MO_n-type units via intermediate building blocks (abundant in a virtual library), by molecular recognition processes for Cu^{2+} centers at the surface/interface of these building blocks, and by selection/addition, to an organized complex mesoscopic ring-shaped structure with a variety of functionalities.[2, 3] The highly symmetrical mesoscopic $\{Mo_{154}\}$ parent ring structure, which in the present case is the primary aim of the self-assembly process, can undergo a variety of modifications by altering the boundary conditions, or in other words, because of environmental influences, as for example, the presence of Cu^{2+} ions. In this context, it is important to realize that assembly processes based on simple linkable units lead preferably to highly symmetrical species,[9, 10] such as rings, corresponding to many observations in cluster chemistry (for general aspects, see also ref. [11]). A relevant aspect in this context is that mesoscopic (i.e. giant) systems can, in spite of a high overall symmetry, exhibit a manifold of highly reactive substructures with related functionalities, for example, on the (large) surface or inside cavities, as in the present case. This feature is noteworthy as the accepted view is that higher symmetry leads to a decrease in structural details and reactivities, which applies, however, to smaller discrete species as well as crystalline systems with macroscopic homogenicity and microscopic translational invariance, but not to discrete mesoscopic molecular-type species. Interestingly, the spherical virus situation also provides a relevant example, as mentioned in most biochemistry textbooks.

Our results show that the molybdenum oxide based wheel-shaped nanoclusters can be considered as nanostructured landscapes with well-defined functional groups.[2, 3] This allows different types of reactions, also catalytic ones, at well-defined positions, among others, 1) the coordination of (activated) ligands including amphiphilic and multiphilic ones even at electron-rich sites with the option of generating unusual surfaces within cavities,[12] 2) the generation of different types of defects (supported as in the present case by relatively high pH values), and 3) as in the present case, the incorporation of metal centers in appropriate cavities. A further perspective based on this work is that reactivities and electron distributions of nanoobjects can be modulated by defect generations as well as by incorporated open-shell heterometal atoms. In the present case, the influence of the Cu^{2+} centers on the distribution of delocalized electrons within compartments can be nicely demonstrated by a shift of the IVCT band from approximately 750 nm of the parent $\{Mo_{154}\}$ anion[3] to around 680 nm for **1a**. The general aspect of this observation is that the change of electron distribution can influence/tune the reactivity and even the catalytic activity of the present nanoobjects, which can show selective oxidations.[13]

Experimental Section

1: Copper powder (0.50 g, 7.87 mmol; Merck, p.a., ⟨63 μm/⟩ 230 mesh American Society for Testing and Materials) and 32 % HCl (7.0 mL, p.a.) were added to a solution of $(NH_4)_6Mo_7O_{24} \cdot 4H_2O$ (18.20 g, 14.73 mmol; p.a.) in H_2O (450 mL) resulting in a color change to blue. The reaction mixture was stirred vigorously for 30 min in an open 500 mL (wide-necked) conical flask. After filtration, $HCOONH_4$ (0.70 g, 11.10 mmol; Aldrich, 97 %) was dissolved in the deep blue filtrate and the solution was kept for 8 days (covered with a watch glass and without stirring) for crystallization. The precipitated small black crystals of **1** were collected by filtration, washed with ice-cold water, and dried over $CaCl_2$ in an inert gas atmosphere. Yield: 1.7 g (8.5 % based on Mo; correct analysis). If 1.0 g copper powder is used, crystals can be obtained after 3–4 days as shown in a later experiment.

Characteristic IR bands for **1** (KBr pellet; 1800–500 cm^{-1}): $\tilde{\nu} = 1616$ (m, $\delta(H_2O)$), 1400 (m, $\delta_{as}(NH_4^+)$), 988 (sh), 971 (m), ca. 940 (sh), 907 (m, ν(Mo=O)), 796 (m), 746 (m), 667 (sh), 630 (s), 554 (s) cm^{-1}; characteristic resonance Raman bands (KBr pellet; $\lambda_e = 1064$ nm; 1000–200 cm^{-1}): $\tilde{\nu} =$ 792 (m), 534 (s), 463 (s), 324 (m-s), 215 (s) cm^{-1}; UV/Vis (solid-state reflectance spectrum measured vs. cellulose as white-standard): $\lambda \approx 500$ (sh), ≈680 (br) nm.

Received: April 20, 2001 [Z16970]
Publication delayed at authors request

[1] a) *Metal Clusters in Chemistry*, *Vol. 1–3* (Eds.: P. Braunstein, L. A. Oro, P. R. Raithby), Wiley-VCH, Weinheim, **1999**; b) *Clusters and Colloids, From Theory to Applications* (Ed.: G. Schmid), Wiley-VCH, Weinheim, **1994**.

[2] a) A. Müller, P. Kögerler, C. Kuhlmann, *Chem. Commun.* **1999**, 1347–1358; b) A. Müller, P. Kögerler, H. Bögge, *Struct. Bonding (Berlin)* **2000**, *96*, 203–236; c) A. Müller, S. K. Das, E. Krickemeyer, *Inorg. Synth.*, in press.

[3] A. Müller, C. Serain, *Acc. Chem. Res.* **2000**, *33*, 2–10.

[4] For interesting aspects of self-assembly processes, see: J.-M. Lehn in *Chemistry for the 21st Century* (Eds.: E. Keinan, I. Schechter), Wiley-VCH, Weinheim, **2000**, pp. 1–7.

[5] Crystal structure analysis of **1**: Space group $C2/m$, $a = 30.490(2)$, $b = 49.580(3)$, $c = 29.112(2)$ Å, $\beta = 96.639(1)°$, $V = 43712(5)$ Å^3, $Z = 2$, $\rho_{calcd} = 2.110$ g cm^{-3}, $\mu = 2.190$ mm^{-1}, $F(000) = 26870$, crystal dimensions: $0.18 \times 0.10 \times 0.10$ mm. Crystals of **1** were removed from the mother liquor and immediately measured at 183 K on a Bruker axs SMART diffractometer (three-circle goniometer with 1 K CCD detector, $Mo_{K\alpha}$ radiation, graphite monochromator). Measurements were performed on a hemisphere with 0.3° ω-scans in three runs with 606, 435, and 230 frames ($\phi = 0$, 88, and 180°) based on a detector distance of 5 cm. Of the 109176 reflections measured ($0.7 < \theta < 25.04°$), 38758 were independent ($R(\text{int}) = 0.092$) and were used in the refinement. An empirical absorption correction on the basis of symmetry-equivalent reflections was carried out with the help of the program SADABS. The structure was solved and refined with the programs SHELXS-97 and SHELXL-93 to $R = 0.0735$ for 24530 reflections with $I > 2\sigma(I)$; max./min. residual electron density: 3.26

  0044-8249/01/11321-4160 $ 17.50+.50/0

and −2.04 e Å^3 (SADABS, SHELXS/L by G. M. Sheldrick, Universität Göttingen, Germany, **1993** and **1997**; structural graphics with DIAMOND 2.1 from K. Brandenburg, Crystal Impact GbR, **1999**). Several individual crystals were measured. Further details on the crystal structure investigation may be obtained from the Fachinformationszentrum Karlsruhe, 76344 Eggenstein-Leopoldshafen, Germany (fax: (+49) 7247-808-666; e-mail: crysdata@fiz-karlsruhe.de), on quoting the depository number CSD-411939.

[6] I. D. Brown in *Structure and Bonding in Crystals, Vol. II* (Eds.: M. O'Keeffe, A. Navrotsky), Academic Press, New York, **1981**, pp. 1–30.

[7] "ESR Spectra of Metal Complexes of the First Transition Series in Low Symmetry Environments": A. Bencini, D. Gatteschi in *Transition Metal Chemistry*, *Vol. 8* (Eds.: B. N. Figgis, G. A. Melson), Marcel Dekker, New York, **1982**, pp. 1–178; J. R. Wasson, P. J. Corvan, W. E. Hatfield, *Inorg. Chim. Acta* **1978**, *27*, 167–171.

[8] The generation of giant wheel-based porous materials and the relevant investigation of their catalytic properties is a separate project investigated together with Prof. F. Schüth (MPI, Mühlheim). The material has to be heated to a well-defined temperature, not too low to guarantee the loss of crystal water, and not too high to avoid cluster deposition. The process is not easy because of the high hydrophilicity of the cluster and the possible release of coordinated H_2O.

[9] A. Müller, S. K. Das, H. Bögge, M. Schmidtmann, A. Botar, A. Patrut, *Chem. Commun.* **2001**, 657–658.

[10] This process can formally (!) be correlated with a general symmetry formalism or symmetry-evolution principle for a quasi-isolated system[11] if only the microworld of the molecular intermediates is considered and not the macroscopic system, for which structure-formation-based precipitation is equivalent to symmetry breaking (cf. H. Genz, *Symmetrie—Bauplan der Natur*, Piper, München, **1987**). The important aspect is that the highly symmetrical species are preferably formed as they are kinetically more inert.

[11] J. Rosen, *Symmetry in Science: An Introduction to the General Theory*, Springer, New York, **1995**.

[12] A. Müller, S. K. Das, C. Kuhlmann, H. Bögge, M. Schmidtmann, E. Diemann, E. Krickemeyer, J. Hormes, H. Modrow, M. Schindler, *Chem. Commun.* **2001**, 655–656.

[13] A. Bielanski, A. Malecka-Lubanska, J. Pozniczek, A. Müller, E. Krickemeyer, E. Diemann, *Bull. Pol. Acad. Sci. Chem.* **2001**, *49*, 85–99.

Structure of $Ca_{13}Cd_{76}$: A Novel Approximant to the $MCd_{5.7}$ Quasicrystals (M = Ca, Yb)**

Cesar Pay Gómez* and Sven Lidin

The compound $Ca_{13}Cd_{76}$ has been synthesized and its structure has been solved from single crystal X-ray diffraction data.[1] The discovery of the stable binary icosahedral quasicrystals $YbCd_{5.7}$ and $CaCd_{5.7}$ opens the doors to new possibilities for understanding quasicrystalline structures.[2, 3] A stable quasicrystalline phase has the obvious advantage that large, single-grain crystals can be grown, which allow detailed investigations of physical properties in the bulk, structural studies with neutron radiation, etc. Most stable quasicrystals are ternary or multinary, and this leads to uncertainties in the occupancy of different atomic sites in the structure. A binary quasicrystal thus offers the additional advantage of simplicity in its structural description. The uniqueness of the $MCd_{5.7}$ (M = Ca, Yb) quasicrystals lies in the combination of these features. Although icosahedral approximants are ubiquitous,[4] the $MCd_{5.7}$ compounds are the only known icosahedral quasicrystals that exhibit both these characteristics.

The structures of the quasicrystal approximants play a key role in understanding quasicrystals, since they are expected to display the same local arrangements as the true quasicrystals, and their long-range order facilitates their structural determination by standard methods. Thus, they provide a link to the underlying mechanism of quasicrystal formation.

Modeling quasicrystals is a very attractive way to predict thermodynamic stability, but large multinary approximants containing several different d- or f-block elements do not easily lend themselves to calculations. $Ca_{13}Cd_{76}$ is even better suited in this context; not only is it a well-ordered, binary system with accurately defined sites for the two types of metal atoms, it is for all practical purposes composed of elements with closed-shell cores.

The classic approximants to the $MCd_{5.7}$ quasicrystals are the long known $CaCd_6$ and $RECd_6$ (RE = rare earth metal) phases;[5, 6] recent investigations conducted at our department, however, show that their true structures have yet not been well characterized. The characterization of $Ca_{13}Cd_{76}$ (or $CaCd_{5.85}$) shows that it is a more closely related approximant to the $MCd_{5.7}$ quasicrystals than any other so far known. The relation between the structures of $CaCd_6$, $Ca_{13}Cd_{76}$, and the icosahedral $MCd_{5.7}$ quasicrystals is implicitly evident from the diffraction patterns of the two approximants; the tenfold symmetry of the patterns is clearly enhanced in $Ca_{13}Cd_{76}$ compared to that of $CaCd_6$ (Figure 1). The recurring structural building blocks seen in the $RECd_6$ phases, $CaCd_6$, and the $RE_{13}(Zn,Cd)_{58}$ phases can be found in $Ca_{13}Cd_{76}$, but in a new, spectacular arrangement.[7, 8] A comparison of the Yb–Cd and the Ca–Cd binary phase diagrams reveals that the systems are very similar; several isostructural phases are present. The compounds $CaCd_{5.7}$ and $YbCd_{5.7}$ were earlier reported in these two systems (as Ca_3Cd_{17} and $YbCd_{5.7}$) but in no other.[5, 9] However, their structures had not previously been characterized. Furthermore, a comparison of atomic radii shows that Yb and Ca are almost identical in size; not even the neighboring lanthanides match the size of Yb better than Ca. The atomic size apparently must be restricted to a narrow span to allow the formation of the $CaCd_{5.85}$, $CaCd_{5.7}$, and $YbCd_{5.7}$ phases. This could explain why no other lanthanides form these phases in combination with Cd, though the 1:6 approximants exist in almost all RE–Cd systems. Furthermore, both Yb and Ca have two s electrons in their outer shell and form divalent ions. All these similarities between the elements make Ca the perfect candidate for the formation of a compound that is next of kin to the $MCd_{5.7}$ quasicrystals.

$Ca_{13}Cd_{76}$ crystallizes in the cubic space group $Pa\bar{3}$ (no. 205), with $a = 25.339(2)$ Å. A convenient way to describe the structure is to identify a unique structural building block and then further describe the cell content in terms of the

[*] C. P. Gómez, Prof. Dr. S. Lidin
Inorganic Chemistry, Arrhenius Laboratory
Stockholm University, 106 91 Stockholm (Sweden)
Fax: (+46) 8-152187
E-mail: cesar@inorg.su.se

[**] This study was financially supported by the Swedish Natural Science Research Council.